Scaling Properties of the Azimuthal Anisotropy in Cu+Cu collisions at $\sqrt{s_{NN}}$ =200 GeV

A. Taranenko, Roy A. Lacey, N.N. Ajitanand, J. Alexander, P. Chung
Chemistry Department, State University of New-York at Stony Brook
(Dated: November 7, 2006)

Detailed measurements of the azimuthal anisotropy (v_2) for identified charged particles (π, K, p) are reported as a function of transverse momentum (p_T) for 0-50% central Cu+Cu collisions at $\sqrt{s_{NN}}$ =200 GeV (Run 5). These high statistics measurements allow further tests of the recently observed universal scaling of baryons and mesons; that is v_2/n_q vs KE_T/n_q gives a single curve for all measured hadrons.

Contents

I. Introduction 2

II. Run and event selections, QA 2
A. Centrality distribution 2
B. Tuning of matching functions for Run5 HardDST's 4

III. Elliptic flow extraction via the reaction plane method 8

IV. Tuning of TOF PID functions 12

V. Elliptic flow of $\pi^{\pm}$, $K^{\pm}$ and p($\bar{p}$) 14

VI. Final Plots for request PHENIX Preliminary 21

References 24

I. INTRODUCTION

Elliptic flow measurements currently play an important role in the many attempts to constrain the transport properties of the QGP produced in energetic heavy ion collisions at RHIC. In ppg062 [1] we reported on the observation of

- eccentricity scaling for charged hadrons produced in both Cu+Cu and Au+Au collisions at $\sqrt{s_{NN}}$ =200 GeV.
- KE_T scaling for identified particles produced in Au+Au collisions and,
- universal scaling of baryons and mesons over a broad range of KE_T for identified particles produced in Au+Au collisions at $\sqrt{s_{NN}}$ =200 GeV.

In this note we extend this earlier work to investigate

- KE_T scaling for identified particles produced in Cu+Cu collisions at $\sqrt{s_{NN}}$ =200 GeV and,
- universal scaling of baryons and mesons for a broad range of KE_T for identified particles produced in Cu+Cu collisions at $\sqrt{s_{NN}}$ =200 GeV.

II. RUN AND EVENT SELECTIONS, QA

The present analysis was performed using minimum-bias Cu+Cu Run5 events ($\sqrt{s_{NN}}$ =200 GeV) from pro.72 and pro.73 versions of the Central Track (CNT) Nano DST's and Hard DST's. A total of $\simeq$ 250 M events from CNT's and $\simeq$ 560 M events from Hard DST's were used subsequent to a $\pm$ 30 cm BBC Z-vertex cut and the rejection of "bad" runs based on QA studies. The HardDST's for Cu+Cu were produced with the lower momentum cut $p \geq 0.6$ GeV/c. Consequently, it was necessary to use CNT's to access the lower p_T results. It is important to note at the outset that the differential $v_2(p_T)$ extracted from CNT's and the Hard DST's are in good agreement over the entire range relevant to this study 0.6-3.0 GeV/c (see below).

The MasterRecalibrator was used to recalibrate the data. The analysis code location in CVS is:
1) CVS:/offline/analysis/v2pidCuCu200/cucu200picodst - compact picoDST's with TOF and EMC PID information
2) CVS:/offline/analysis/v2pidCuCu200/v2hadron - v_2 analysis using picoDST's
Only full field runs for which the number of events was greater than 250 k were used. In addition we rejected runs based on QA studies as follows:

A. Centrality distribution

For each run the centrality distribution was fitted with a constant (p0) and the χ^2/ndf was calculated. Fig. 1 gives an example of runs having a "bad" centrality distribution. We rejected runs with $\chi^2/ndf > 3$, see Fig. 2.

The following runs were excluded based on reaction centrality QA studies: 150513, 150654, 150731, 151443, 151461, 151827, 151915, 152083, 152085, 152088, 152098, 152099, 152101, 152130, 152135, 152136, 152169, 152230, 152349, 152995, 153002, 153010, 153516, 153519, 153523, 153525, 153576, 153616, 153651, 153652, 154650, 155078, 155113, 155118, 156604, 156605, 156621, 157097, 157112, 158027, 158469, 158661, 158664, 158973, 158975, 158979, 158987, 158993, 158994, 159112, 159117, 159145, 159275, 159278.

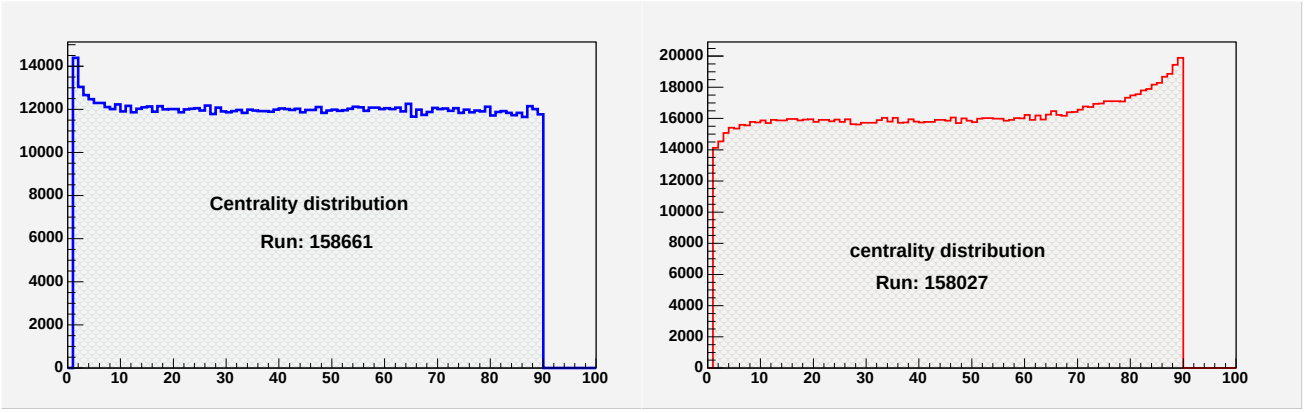

FIG. 1: An example of runs with "bad" centrality distribution. Cu+Cu at $\sqrt{s_{NN}}$ =200 GeV

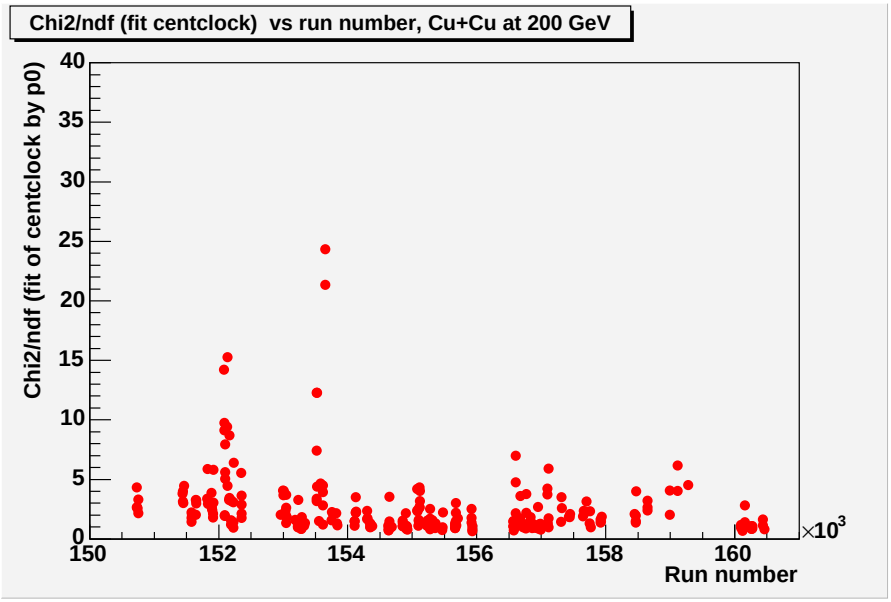

FIG. 2: χ^2/ndf of the fit of centrality by clock distribution as a function of run number (Cu+Cu 200 GeV, Run5)

B. Tuning of matching functions for Run5 HardDST's

In the CNT nanoDST's the normalized differences between the track model projections and hits are stored in terms of n-sigma matching distributions (pc3sdz, pc3sdphi, tofsdz, tofsdphi, ...etc). In the ideal case, the residual n-sigma distributions should have a width of one and should be centered at zero independent of particle momentum , charge and reaction centrality. The re-calibrator for matching in Run 5 Cu+Cu (200 GeV) appeared to work well and we did not find any indication for refining the corrections. On the other hand, the re-calibrator could not be applied to the HardDST's because of the absence of the requisite raw data variables in this data set. This being the case, we repeated the calibration for matching functions for the Hard DST's. A representative set of results from this re-calibration is shown in Figs. 3 and 4. They show the momentum dependence of the mean and width of several matching n-sigma distributions before (left panel) and after (right panel) recalibration. The right panels of the figure speaks to the quality of these recalibrations.

The stability of the re-calibration over run number was also investigated and found to be robust. This is illustrated in Fig. 5 where we show the run-by-run variation of the mean and sigma of the n-sigma matching distributions for the TOF detector. They show good stability across runs.

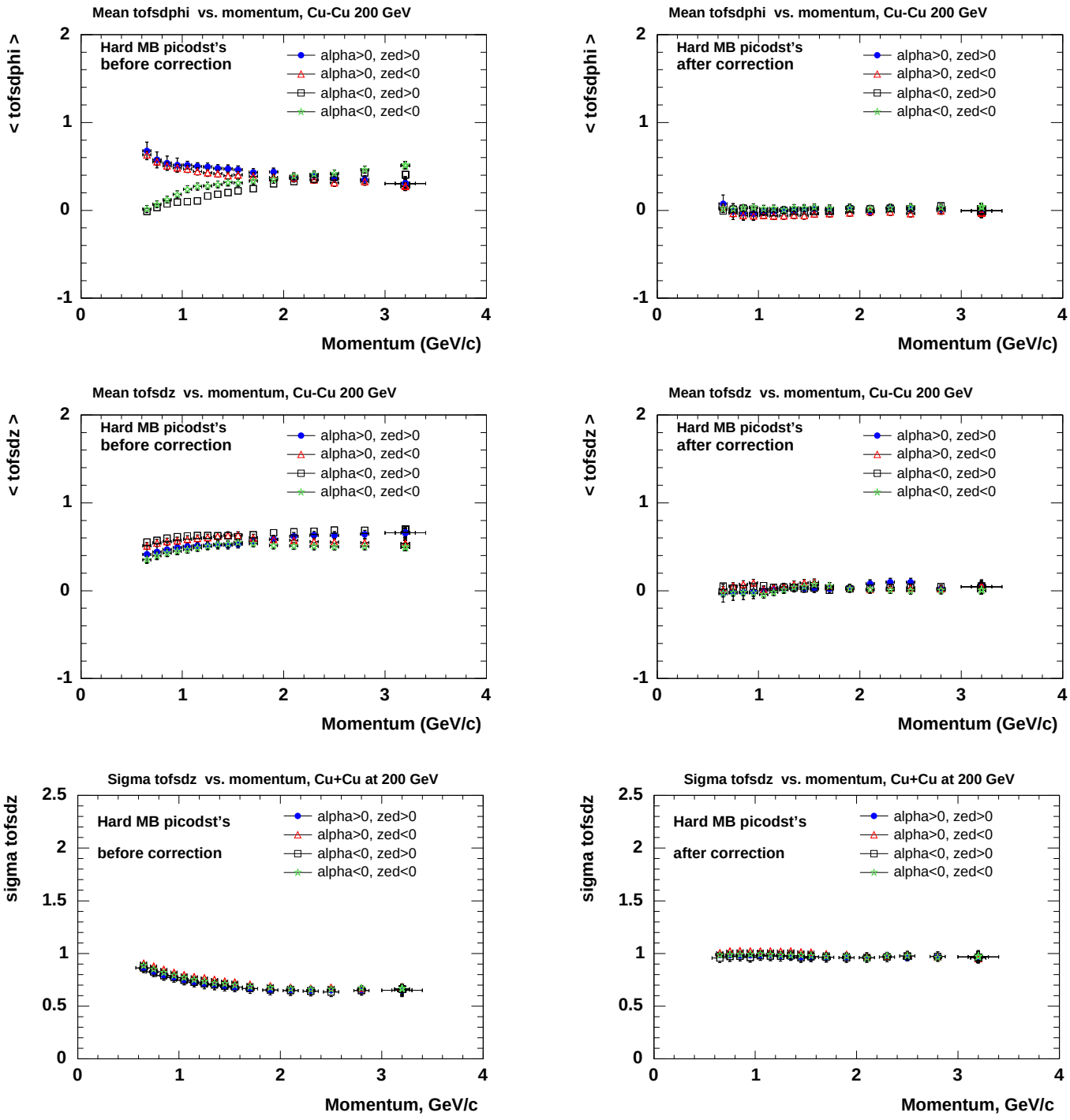

FIG. 3: Mean and width of the residual matching distribution tofs$\Delta\phi$ and tofsΔz as a function of momentum for positive and negative particles before correction (left panel) and after correction (right panel).

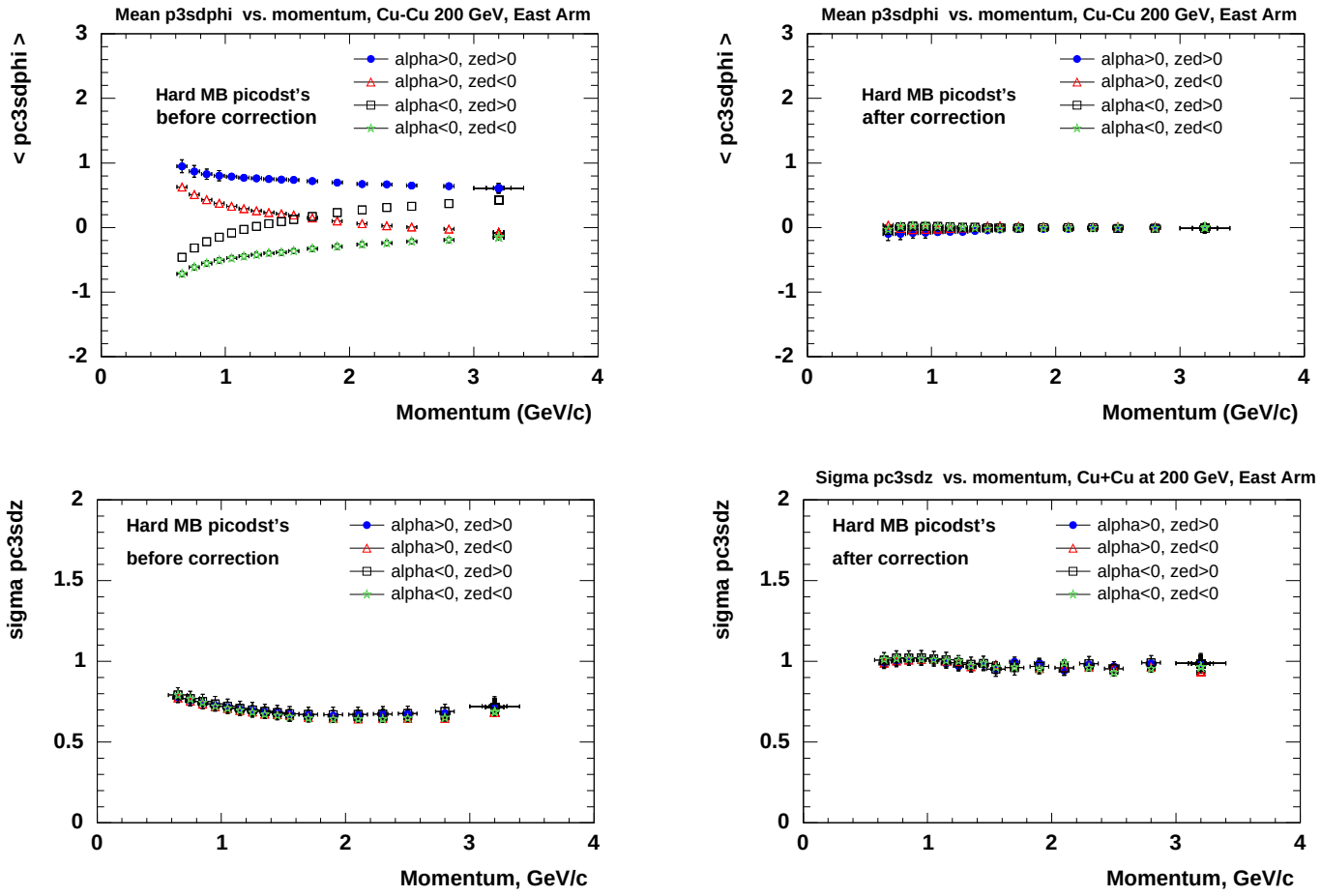

FIG. 4: Mean and width of the residual matching distribution pc3s$\Delta\phi$ and pc3sΔz as a function of momentum for positive and negative particles before correction (left panel) and after correction (right panel).

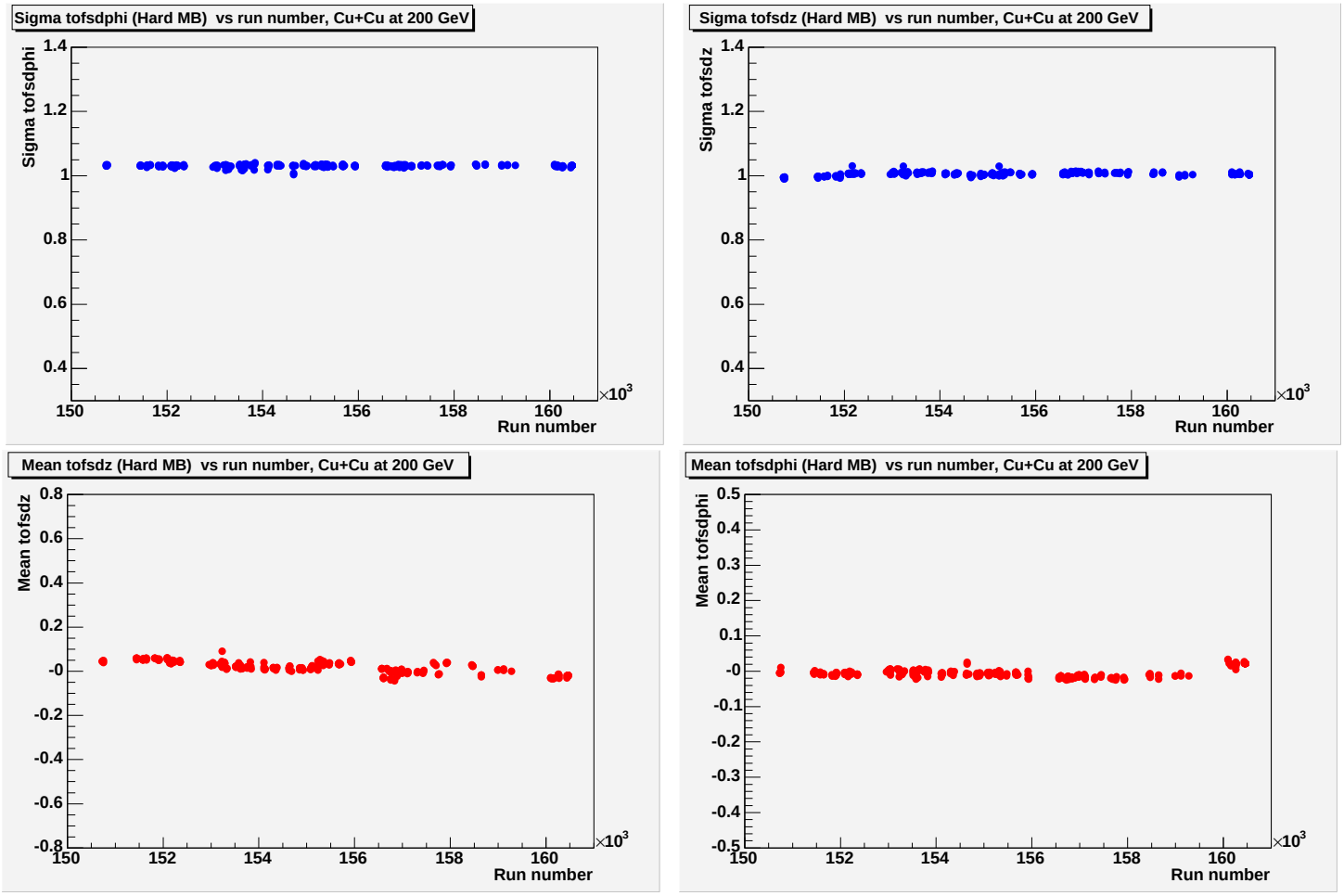

FIG. 5: Mean and width of the residual matching distribution tofs$\Delta\phi$ and tofsΔz as a function of run number after corrections.

III. ELLIPTIC FLOW EXTRACTION VIA THE REACTION PLANE METHOD

The reaction plane method of analysis is not only straightforward, it is commonly used in many PHENIX analysis'. It involves the determination of the azimuth of the reaction plane Ψ followed by the construction of an event-averaged azimuthal distribution for particles relative to the event plane $(\Psi - \phi)$. A subsequent Fourier analysis of this distribution gives the second order Fourier coefficient $(\langle\cos(2(\Psi - \phi)\rangle)$ which is an estimate of the raw azimuthal anisotropy. A requisite correction of this anisotropy for reaction plane dispersion leads to an estimate of the "true" azimuthal anisotropy.
The azimuth of the event-by-event reaction planes were obtained directly from the CNT nanoDST's (BBC south and north reaction planes: rp10 and rp11, and the combined reaction plane rp12). The earlier reaction plane calibration for Cu+Cu ($\sqrt{s_{NN}}$ =200 GeV), done during QM2005, is currently not working for the recently produced Cu+Cu data. This is because the calibration of the BBC and the centrality calibration was changed. A recent calibration was done only for a limited number of runs.

We have performed a re-calibration of the reaction plane using the official reaction plane re-calibrator using the full statistics of the Cu+Cu data. That is, all 320 runs were used. Fig. 6 shows representative distributions for the azimuth of the reaction plane (rp10, rp11 and rp12) for run 157115. The left and right panels show distributions before and after re-calibration respectively. The right panels show rather flat reaction planes as they should be. Rather careful checks were also

made to ensure good quality assurance. For example, the distribution of the reaction plane azimuths were checked for each centrality to ensure that they were flat (see Fig.7 as an example of this). As illustrated in Fig. 7, the calibration of the reaction plane is rather good; they do not require any additional corrections for 10% bins in reaction centrality both.

The correction factors for reaction plane dispersion were estimated at each centrality using the "Ollitrault - Voloshin" method [2, 3] from the measured distribution of the relative angle between sub-events $\Delta\phi_R = \Psi_N - \Psi_S$, where Ψ_N is the azimuth of the reaction plane determined in BBC north and Ψ_S is the azimuth of the reaction plane determined in BBC south. In order to determine the resolution parameter χ_I and corresponding reaction plane dispersion σ_{RP} we fitted this distribution by Eq.2.

$$\frac{dN}{d\Delta\phi_R} = \frac{e^{-\chi_I^2}}{2}\left[\frac{2}{\pi}(1+\chi_I^2) + z(I_0(z)+L_0(z)) + \chi_I^2(I_1(z)+L_1(z))\right] \quad (1)$$

were z=$\chi_I^2 cos(\Delta\phi_R)$ and L_0 and L_1 are modified Struve functions, see [3] for details.

In addition the correction factors for reaction plane dispersion were estimated at each centrality as;

$$\sigma_{RP} = \sqrt{2\cdot < cos2(\Psi_N - \Psi_S) >} \quad (2)$$

where Ψ_N is the azimuth of the reaction plane determined in BBC north and Ψ_S is the azimuth of the reaction plane determined in BBC south. No appreciable difference between these two methods for the estimation of the reaction plane resolution for Cu+Cu was found as illustrated in Fig. 8.

An important step was to check the p_T dependence of the elliptic flow for charged hadrons for the same centralities reported in PPG062. To do this, the following cuts were used for event and track selection:

- vertex cut $\|\text{BBCZ}\| < 30$ cm
- Cuts: 2 "radial" matching cut: PC3 (matching were recalibraited for HardDST's, see next section).

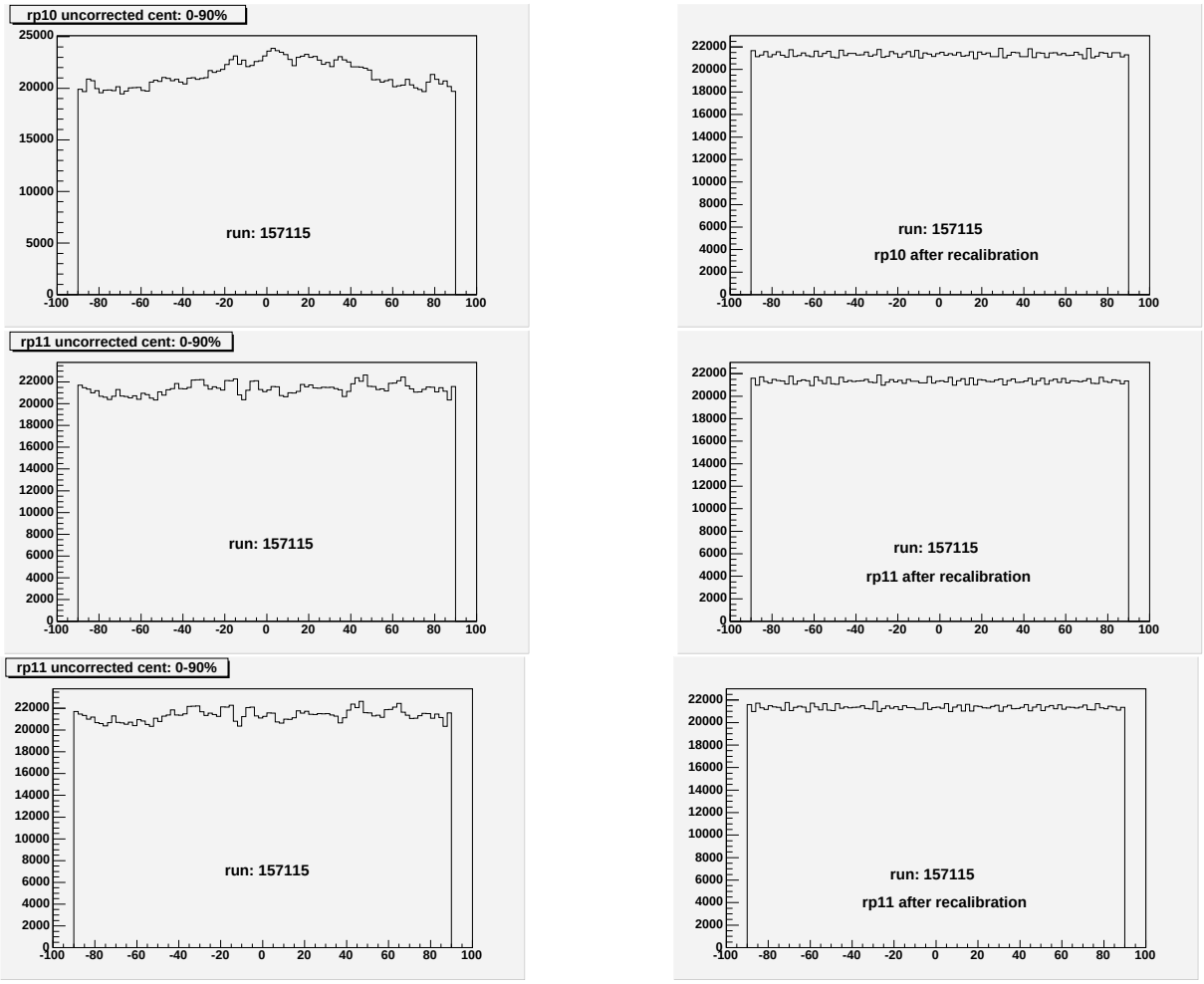

FIG. 6: Distributions of the azimuth of the reaction planes (rp10, rp11, rp12) for min.bias Cu+Cu at $\sqrt{s_{NN}}$ =200 GeV events with "old" (left panel) and new rp calibration (right panel)

- Track quality: 31 or 63

The results are presented in Fig. 9 for the following bins in collision centrality: 0-10%, 10-20%, 20-30% and 30-40%. As one can see from Fig. 9, there is good agreement between the v_2 values obtained using CNT's and HardDST's as well as with the published results from PPG062 [1, 4–6].

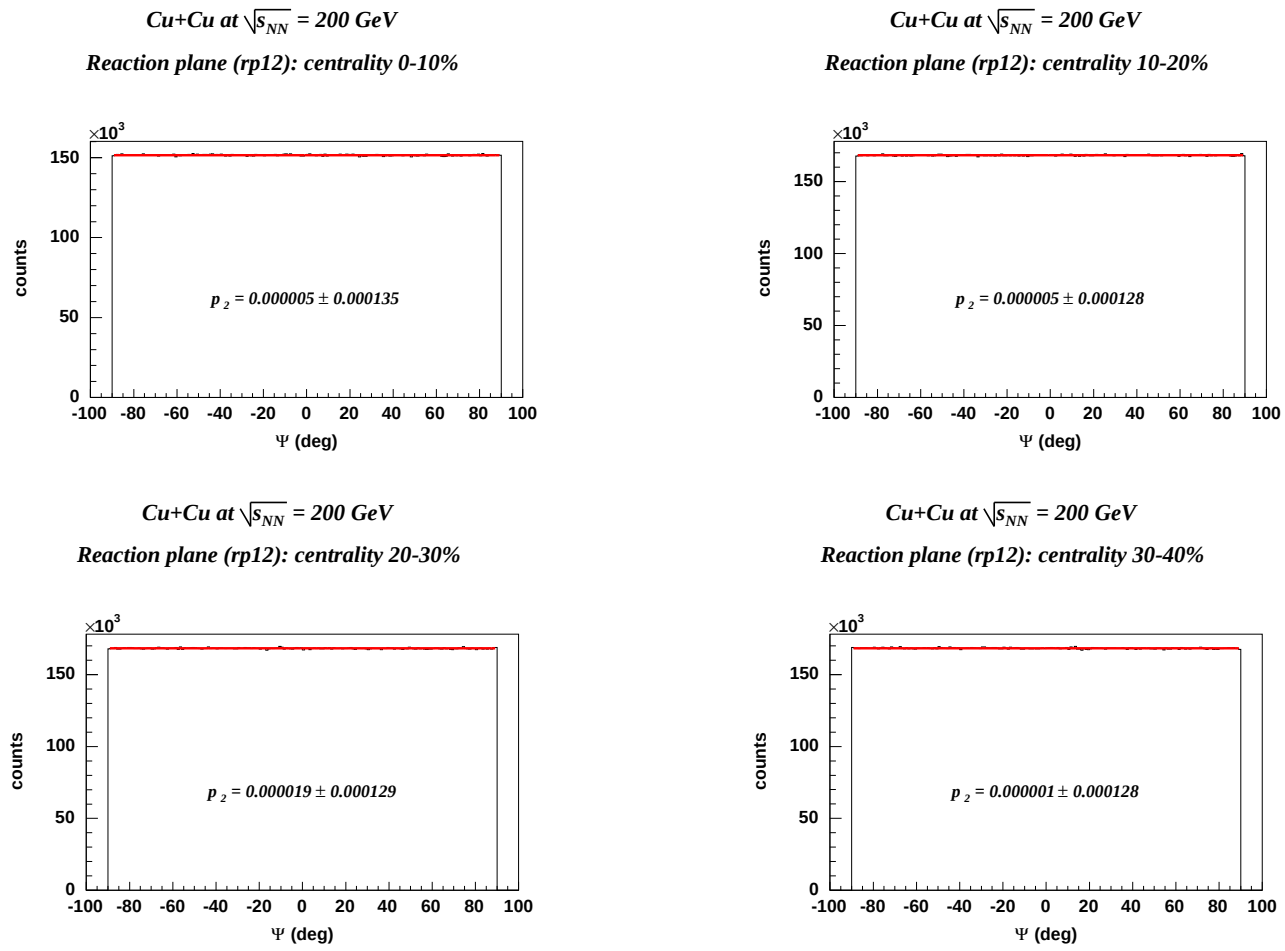

FIG. 7: Distribution of the azimuth of the reaction plane (rp12) for different bins in reaction centrality for Cu+Cu at $\sqrt{s_{NN}}$ =200 GeV

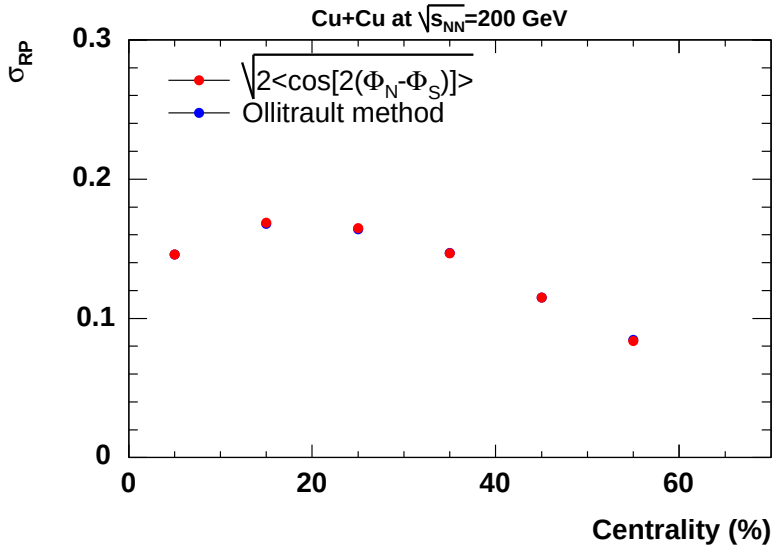

FIG. 8: Centrality dependence of the correction factor (σ_{RP}) for reaction plane dispersion.)

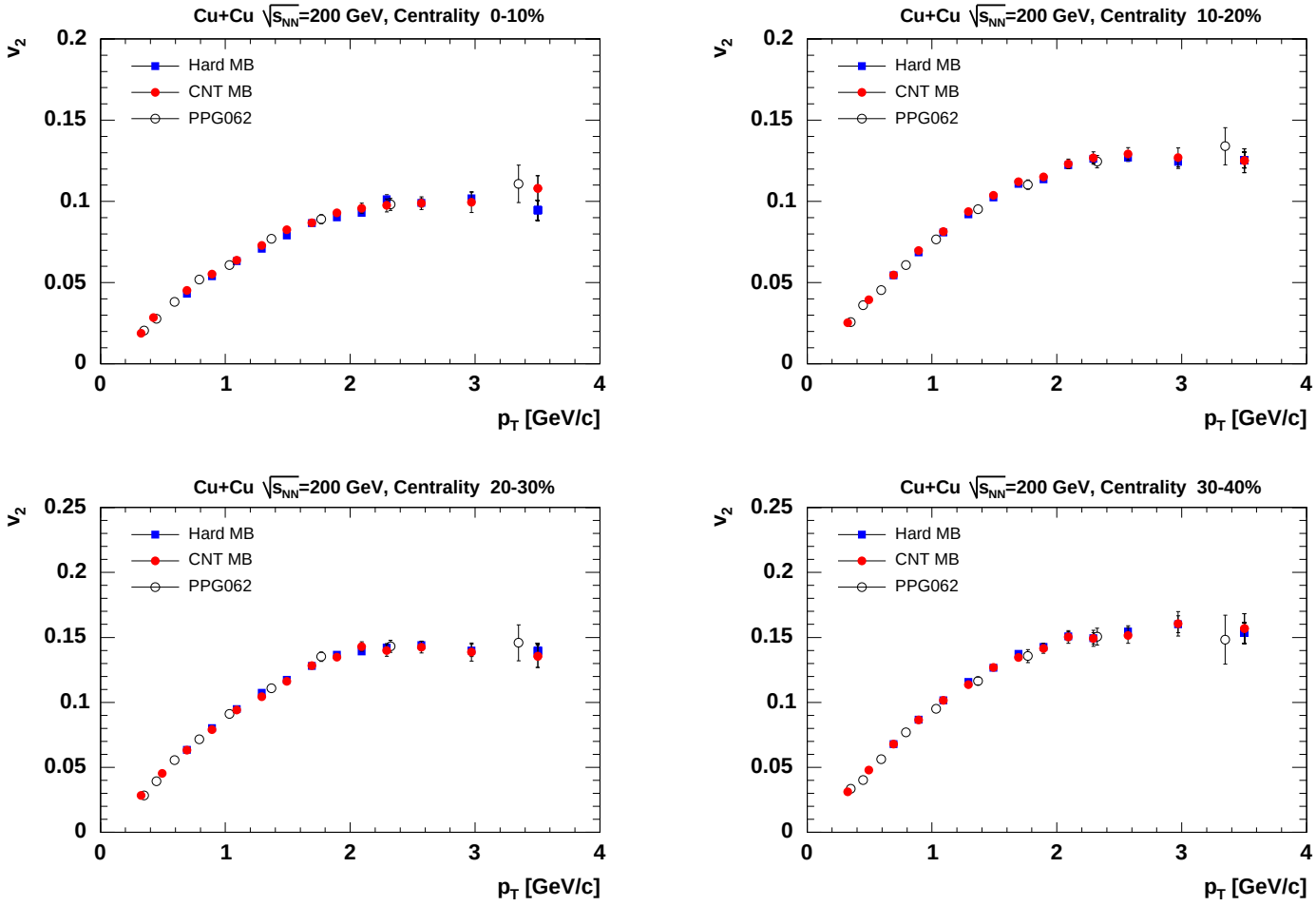

FIG. 9: p_t dependence of v_2 of charged hadrons from Cu+Cu collisions at 200 GeV for different bins in reaction centrality. The solid circles and boxes represent the results from the present analysis obtained using CNT's and HardDST's. Black open circles show the results from the PPG062 [1, 4–6].

IV. TUNING OF TOF PID FUNCTIONS

Since the present analysis is based on charged particle-identification using the TOF detector, we performed detailed checks of the TOF calibration in Cu+Cu 200 GeV (Run5). First we plotted the run-by-run dependence of the T0 offset (position of the peak of the distribution tof-time (expected for π) for momentum range 0.8-1.5 GeV/c, see left panel of Fig. 10. As one can see, it was necessary to calibrate the T0 offset of a number of runs. The following group of runs were found to be uncalibrated and required T0 offset correction of the order of $\simeq$ 7.8 ns: 150553, 150731, 150754, 151898, 152136, 152195, 153225, 153336, 153576, 155076, 155311, 157443, 150555, 150732, 151439, 152094, 152169, 152224, 153226, 153516, 153614, 155113, 155312, 158179, 150556, 150733, 151461, 152098, 152192, 152225, 153277, 153519, 153616, 155118, 155314, 158450, 150659, 150743, 151577, 152130, 152193, 152349, 153279, 153520, 154106, 155276, 157157, 150660, 150753, 151582, 152135, 152194, 152356, 153285, 153525, 154129, 155277, 157427.

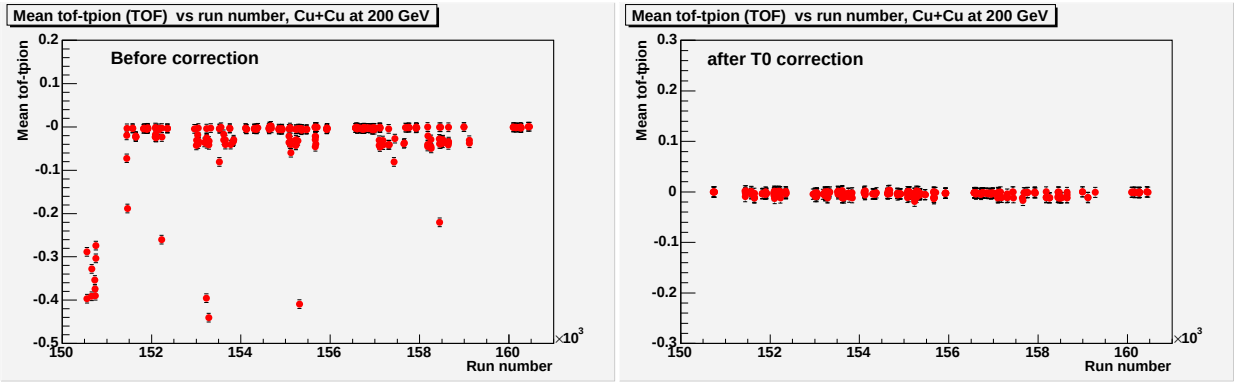

FIG. 10: Mean of the distribution tof-time(expected for π) with momentum 0.8-1.5 GeV/c detected in TOF detector as a function of run number before correction (left panel) and after correction (right panel).

Fig. 11 shows the run-by-run dependence of the timing resolution of the TOF detector and the position of the mass-squared peak for protons and anti-protons after applying the correction for the T0 offset and recalculating mass^2 of particles detected in the TOF. As one can see, the timing resolution is rather good 135-145 ps for the selected runs. Equally important is the fact that there is no splitting in the mass^2 peaks for protons and anti-protons; a good sign which indicates that the momentum re-calibrator is working correctly.

However, one still needs to correct the PID functions, ie. the n-sigma distributions for charged pions, kaons and (anti-)protons, see Fig. 12. For each particle we found the dependence of the mean and width of mass^2 distributions and rebuild PID functions: isPi (isK,isP) =(m^2(tof)-m^2(meas))/σ_{m^2}

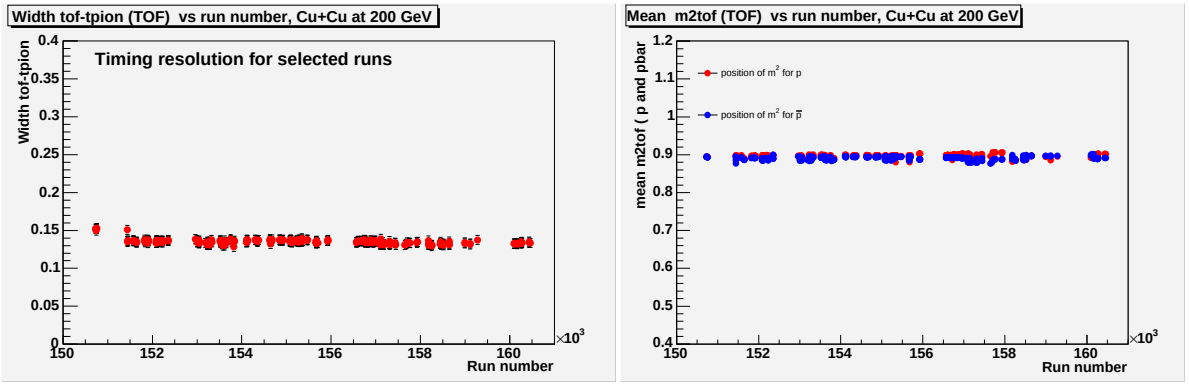

FIG. 11: Left panel: Timing resolution of TOF detector as a function of run number and Right panel: position of calibraited mass-square peak for protons and anti-protons as a function of run number after applying correction for T0 offset and recalculating mass^2.

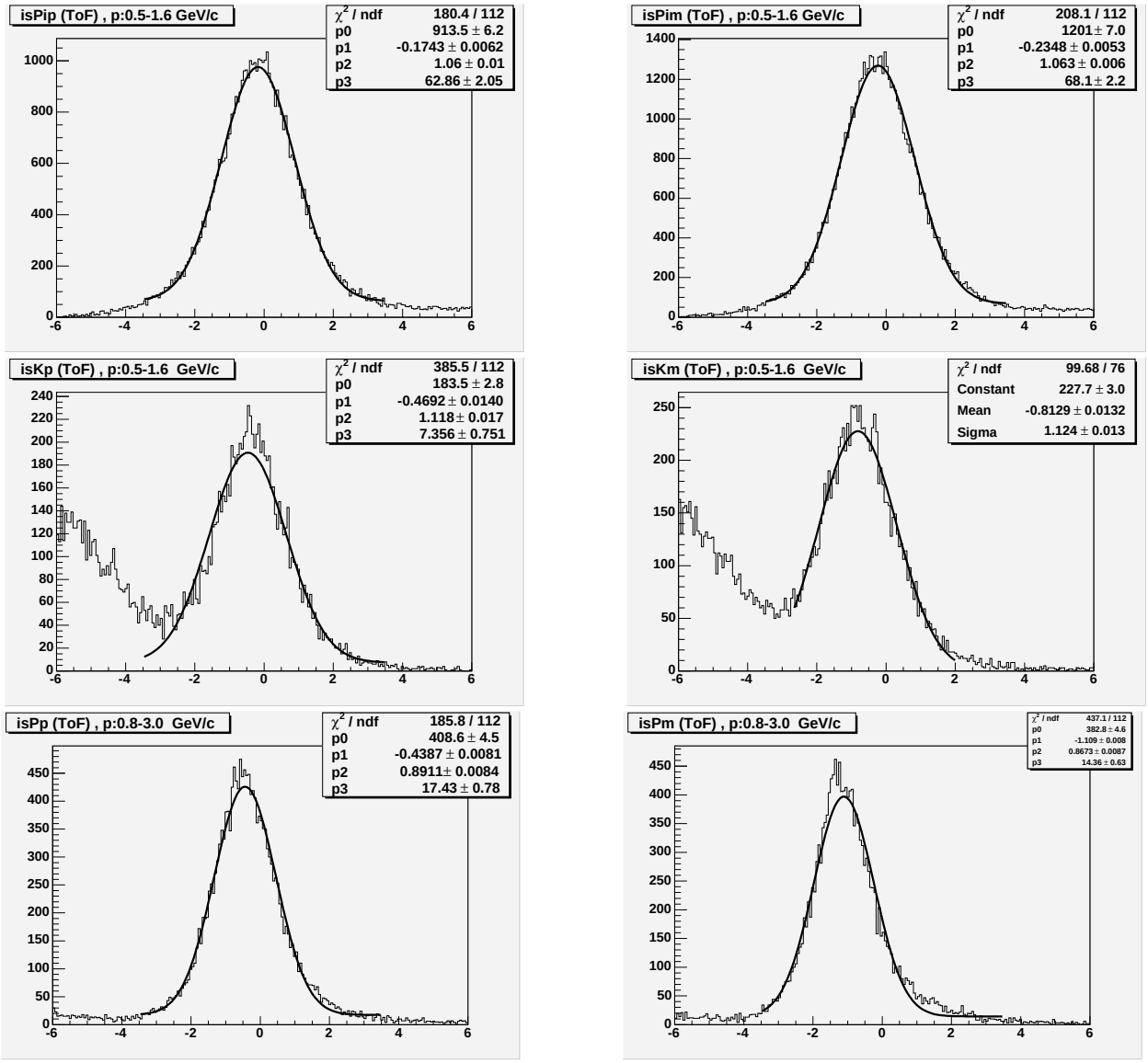

FIG. 12: An example of PID n-sigma distributions : isPi, isK and isP for positive and nnegative particles for Run 157115

V. ELLIPTIC FLOW OF $\pi^{\pm}$, $K^{\pm}$ AND P($\bar{p}$)

The following cuts were used for selection of $\pi^{\pm}$, $K^{\pm}$ and p($\bar{p}$) using TOF detector.

- Cuts: 2.5 σ "radial" matching cut: TOF + PC3
- Track quality: 31 or 63

With standard TOF PID technique we can separate pions and kaons with 2σ PID cut up to p_T=1.8 GeV/c and we can extend the upper limit up 2.5 GeV./c using the asymmetric PID cuts. Protons can be separated from mesons up p_T=3.2 Gev/c with 2σ PID cut, see Fig. 13 as an example, and we can extend the upper limit up 3.8 GeV./c using the asymmetric PID cuts. Left part of Fig. 14 shows the resulting P_T dependence of elliptic flow signal v_2 of $\pi^{\pm}$, $K^{\pm}$ and p($\bar{p}$) from 0-50% central Cu+Cu at $\sqrt{s_{NN}}$ =200 GeV collisions. The right part of Fig. 14 shows the same data plotted in scaled variables: v_2/n_q vs KE_T/n_q, where KE_T is transverse kinetic energy of the particle.

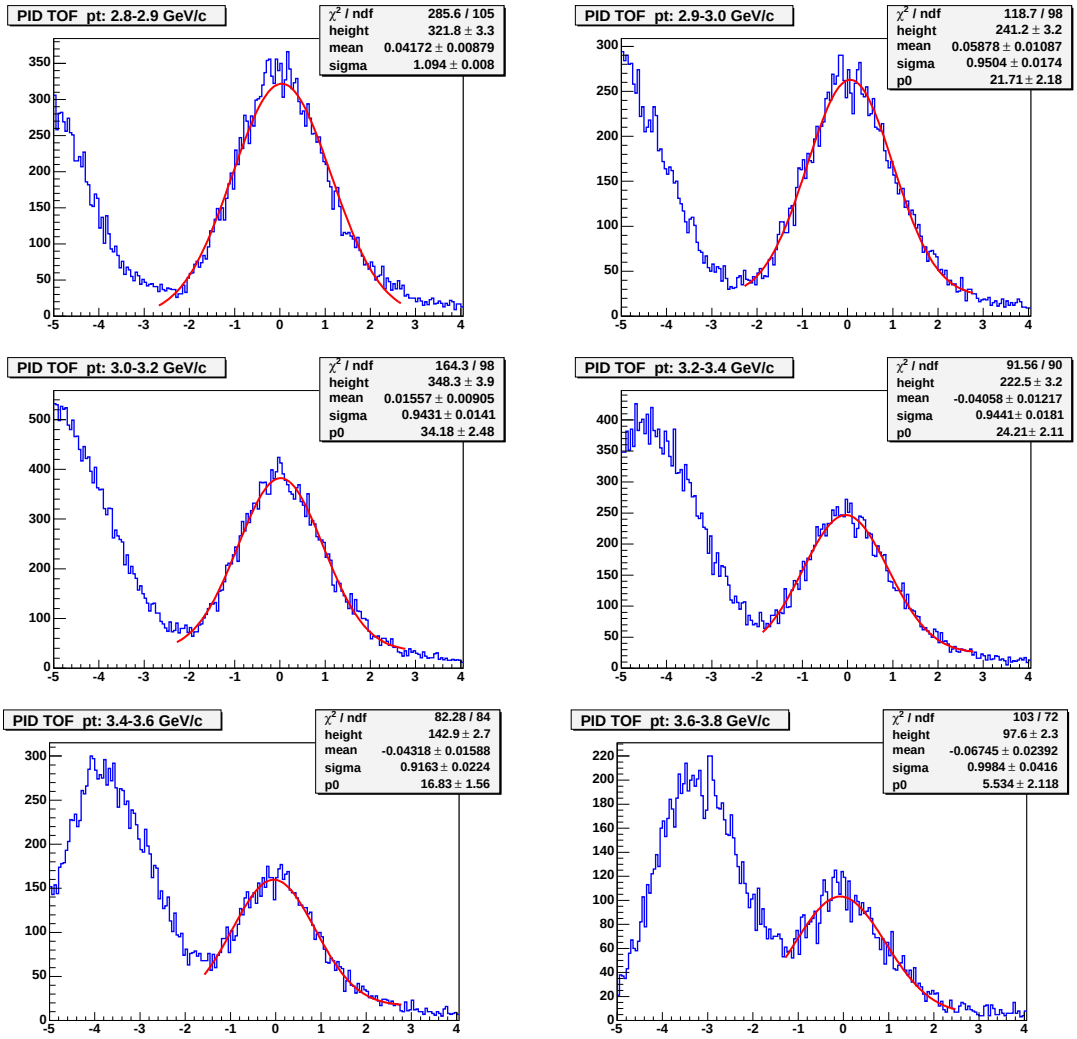

FIG. 13: n-sigma distribution isP (TOF) for pt=2.8-3.8 GeV/c

Event plane resolution for such wide centrality bin: 0-50% was calculated for each particle by averaging the event plane resolution obtained in 10% centrality bins weighting with the yield of π, K

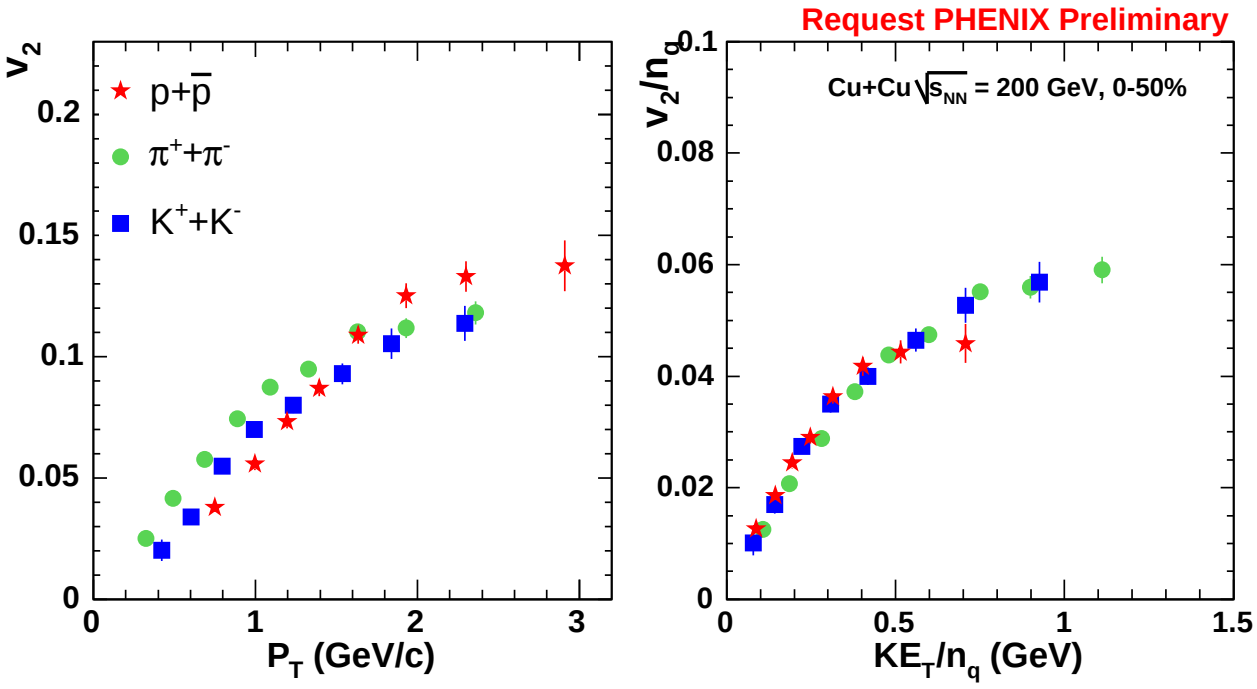

FIG. 14: Left part shows the resulting P_T dependence of elliptic flow signal v_2 of $\pi^{\pm}$, $K^{\pm}$ and p($\bar{p}$) from 0-50% central Cu+Cu at $\sqrt{s_{NN}}$ =200 GeV collisions. The right part shows the same data plotted in scaled variables: v_2/n_q vs KE_T/n_q, where KE_T is transverse kinetic energy of the particle.)

and protons in each centrality. The results of this procedure is presented in the Table.1. The number of π, K and protons for each centrality bin was selected by applying 2 σ PID cut and selecting the following momentum range: 0.25-1.8 GeV/c for $\pi^{\pm}$, 0.3-1.7 GeV/c for $K^{\pm}$ and 0.5-3.5 Gev/c for (anti-)protons. The resulting event plane resolutions are the following: σ_{RP} (π) = 0.1529 for charged pions, σ_{RP} (K) =0.1531 for charged kaons and σ_{RP} (p)=0.1531 for (anti-)protons.

TABLE I:

Centrality	σ_{RP}	N($\pi^{\pm}$)	N($K^{\pm}$)	N($p,\bar{p}$)
0-10%	0.1457	47616825	3164612	3857184
10-20%	0.1662	38524792	2503199	3112529
20-30%	0.1658	27006614	1705937	2160812
30-40%	0.1472	18645710	1141163	1481448
40-50%	0.1198	12329682	726327	959847

The error bars in Fig.14 are statistical only. In order to estimate the systemic errors we studied p_T dependence of elliptic flow of charged hadrons 0-50% central collisions measured with respect to the North BBC reaction plane , South BBC reaction plane and combined (S+N) reaction plane. The difference between results obtained with combined reaction plane and single BBC North and South is of the order of $\simeq$ 2.5% for the centrality 0-50%, see Fig. 15.

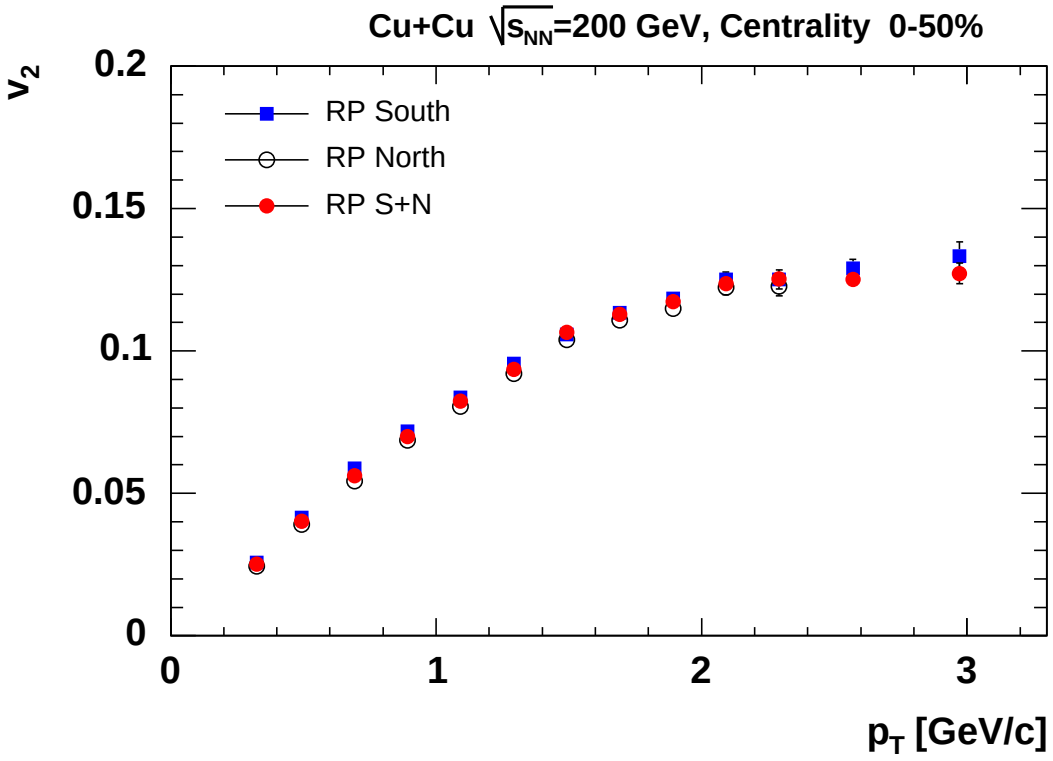

FIG. 15: P_T dependence of elliptic flow signal v_2 of charged hadrons from 0-50% central Cu+Cu collisions measured with respect to the North BBC reaction plane , South BBC reaction plane and combined (S+N) reaction plane. particle.)

Also we checked run dependence of elliptic flow signal of charged hadrons and the v_2 vs p_T values obtained for seven different group of runs are differ less than $< 3\%$, see Fig. 16. Based on these studies we estimate the systematic error to be of the order of $\simeq 4\%$.

As one can see from the right part of Fig. 14 the elliptic flow of $\pi^{\pm}$, $K^{\pm}$ and p($\bar{p}$) from 0-50% central Cu+Cu collisions at $\sqrt{s_{NN}}$ =200 GeV collisions folow the recently observed v_2/n_q vs KE_T/n_q scaling and we know that elliptic flow of charged hadrons scaled by integral v_2 (which is proporional to initial eccentricity) is independent on reaction centrality and colliding systems. We can take the Au+Au v_2 values for $\pi^{\pm}$, $K^{\pm}$ and p($\bar{p}$) for a given centrality and scale by integral v_2 of charged hadrons and plot togather with scaled values from Cu+Cu, see Fig. 17. The v_2 values for $\pi^{\pm}$, $K^{\pm}$ and p($\bar{p}$) from 0-50% central Au+Au at $\sqrt{s_{NN}}$ =200 GeV collisions (Run4) were taken from H. Masui analysis [7].

The next important step was to make the comparison of the p_T dependence of the elliptic flow for $\pi^{\pm}$, $K^{\pm}$ and p($\bar{p}$) with previous PHENIX Preliminary results from QM2005 analysis of H. Masui [6]. These measurements were done for minimum bias Cu+Cu collisions. We also analyzed minimum bias collisions with the same set of cuts. The resulting p_T dependence dependence of v_2 of $\pi^{\pm}$, $K^{\pm}$ and p($\bar{p}$) is plotted in Fig. 18. Fig. 19-21 show the comparison with QM2005 Preliminary results for each particle species.

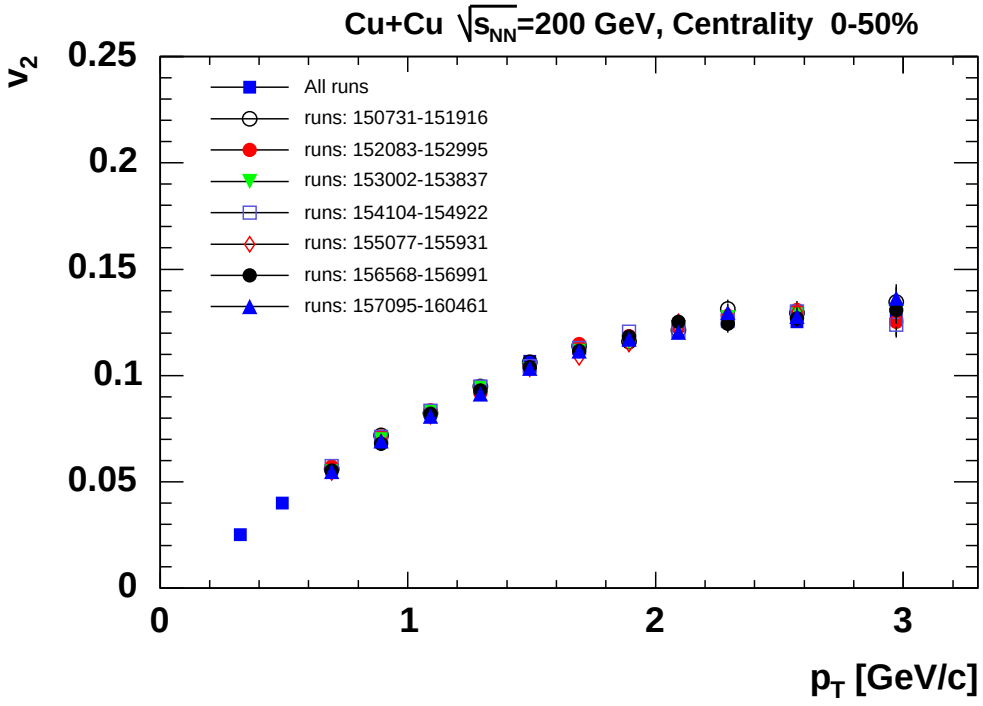

FIG. 16: P_T dependence of elliptic flow signal v_2 of charged hadrons from 0-50% central Cu+Cu collisions measured with respect to the combined (S+N) reaction plane for seven group of runs. . particle.)

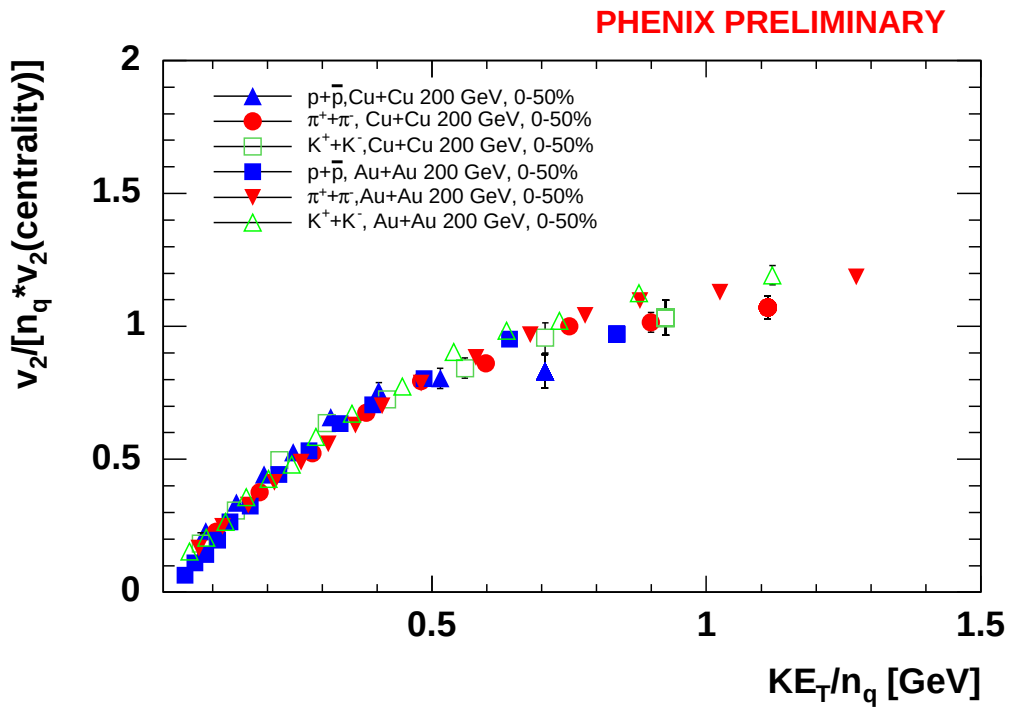

FIG. 17: v_2/n_q vs KE_T/n_q for $\pi^{\pm}$, $K^{\pm}$ and p($\bar{p}$) from central Cu+Cu and Au+Au collisions at $\sqrt{s_{NN}}$ =200 GeV scaled by the integral elliptic flow of charged hadrons measured in pt range 0.3-3.0 GeV/c)

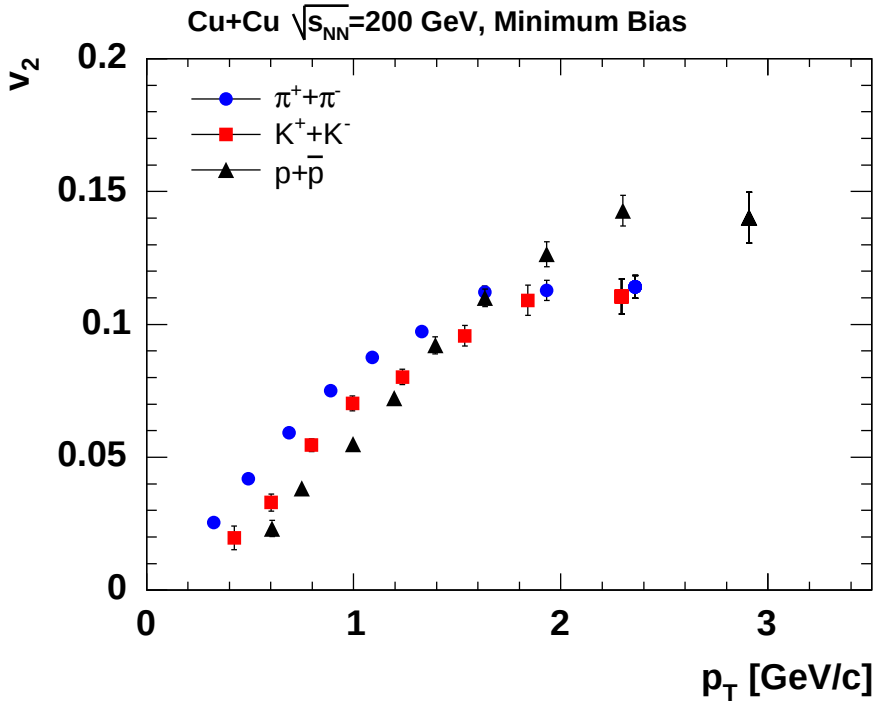

FIG. 18: p_T dependence of the elliptic flow of $\pi^{\pm}$, $K^{\pm}$ and p($\bar{p}$) from the minimum bias Cu+Cu collisions at $\sqrt{s_{NN}}$ =200 GeV

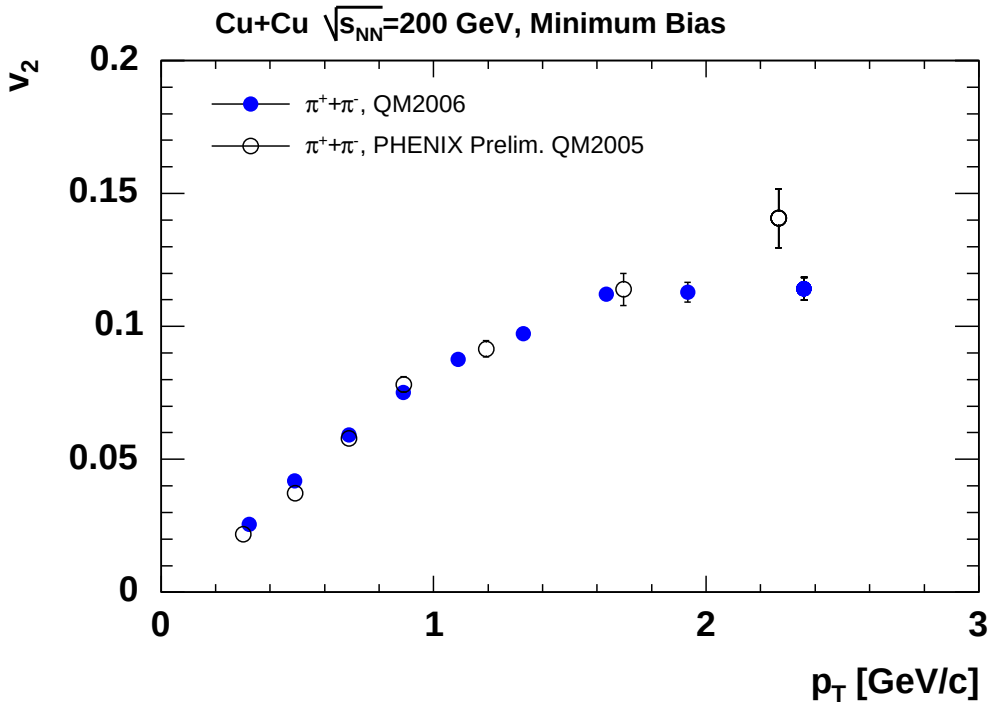

FIG. 19: p_T dependence of the elliptic flow of the charged pions $\pi^{\pm}$ from the minimum bias Cu+Cu collisions. Open symbols represent the PHENIX Preliminary results from QM2005 [6] and the solid symbols the results of the present analysis. at $\sqrt{s_{NN}}$ =200 GeV

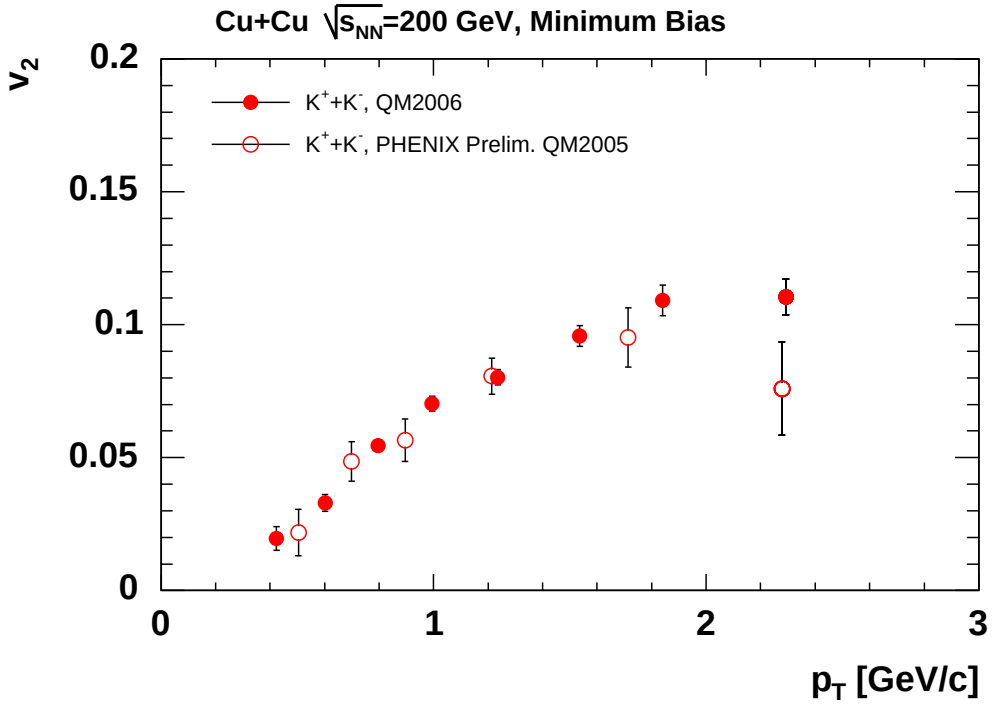

FIG. 20: p_T dependence of the elliptic flow of charged kaons $K^{\pm}$ from the minimum bias Cu+Cu collisions. Open symbols represent the PHENIX Preliminary results from QM2005 [6] and the solid symbols the results of the present analysis. at $\sqrt{s_{NN}}$ =200 GeV

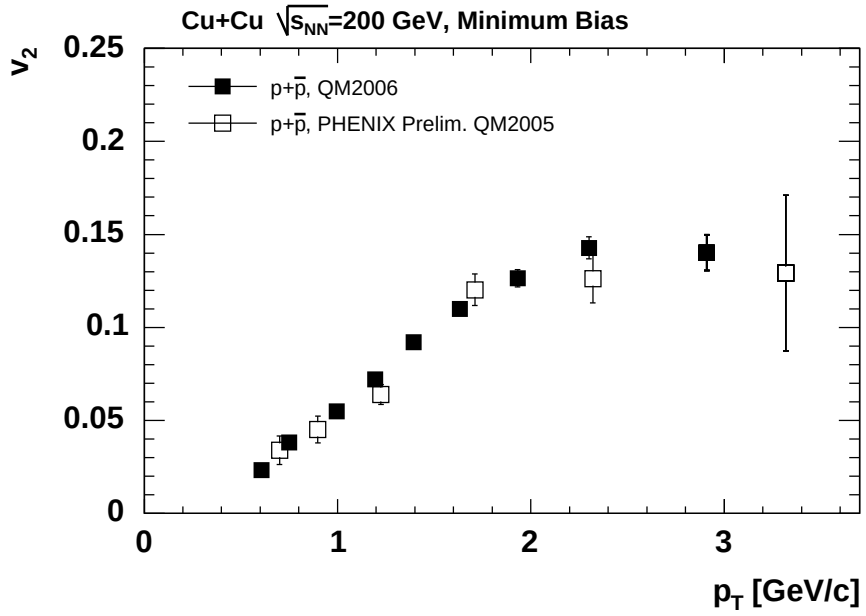

FIG. 21: p_T dependence of the elliptic flow of (anti-)protons p$\bar{p}$ from the minimum bias Cu+Cu collisions. Open symbols represent the PHENIX Preliminary results from QM2005 [6] and the solid symbols the results of the present analysis. at $\sqrt{s_{NN}}$ =200 GeV

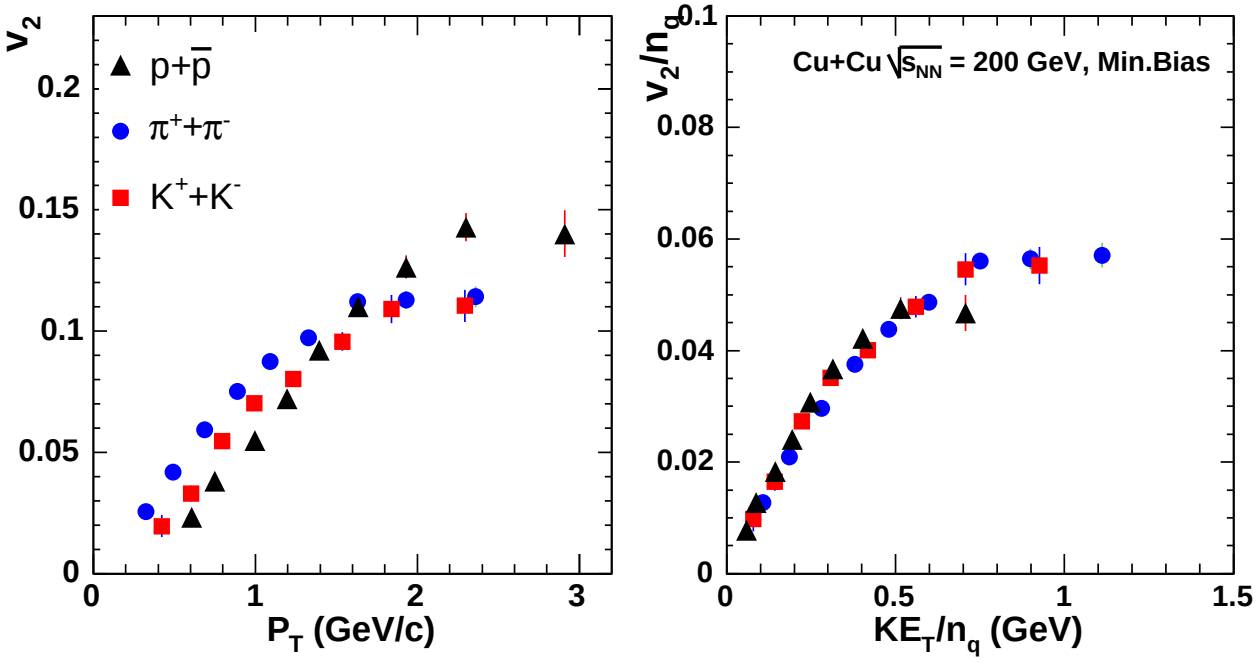

FIG. 22: Left part shows the resulting P_T dependence of elliptic flow signal v_2 of $\pi^{\pm}$, $K^{\pm}$ and p($\bar{p}$) from the minimum bias Cu+Cu collisions at $\sqrt{s_{NN}}$ =200 GeV. The right part shows the same data plotted in scaled variables: v_2/n_q vs KE_T/n_q, where KE_T is transverse kinetic energy of the particle.)

VI. FINAL PLOTS FOR REQUEST PHENIX PRELIMINARY

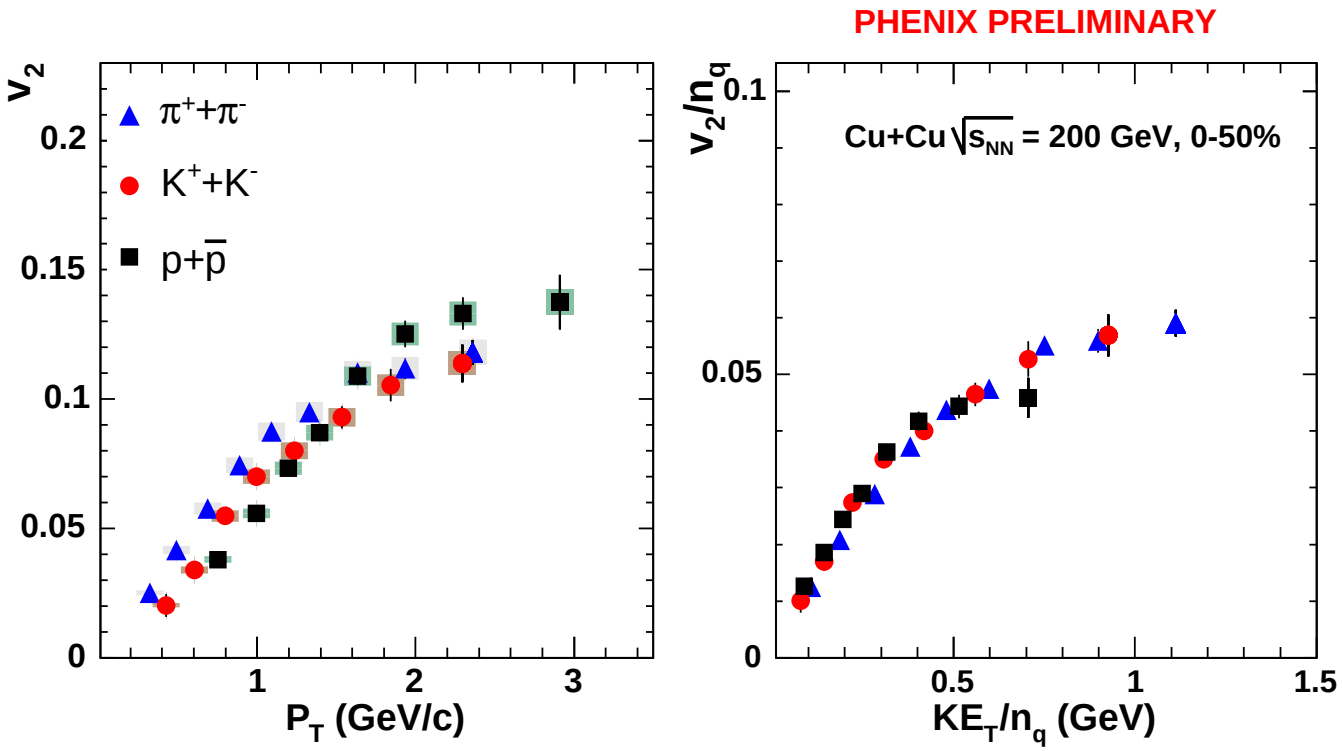

FIG. 23: Left part of Fig. 13 shows the resulting P_T dependence of elliptic flow signal v_2 of $\pi^{\pm}$, $K^{\pm}$ and p($\bar{p}$) from 0-50% central Cu+Cu at $\sqrt{s_{NN}}$ =200 GeV collisions. The right part of Fig. 13 shows the same data plotted in scaled variables: v_2/n_q vs KE_T/n_q, where KE_T is transverse kinetic energy of the particle.)

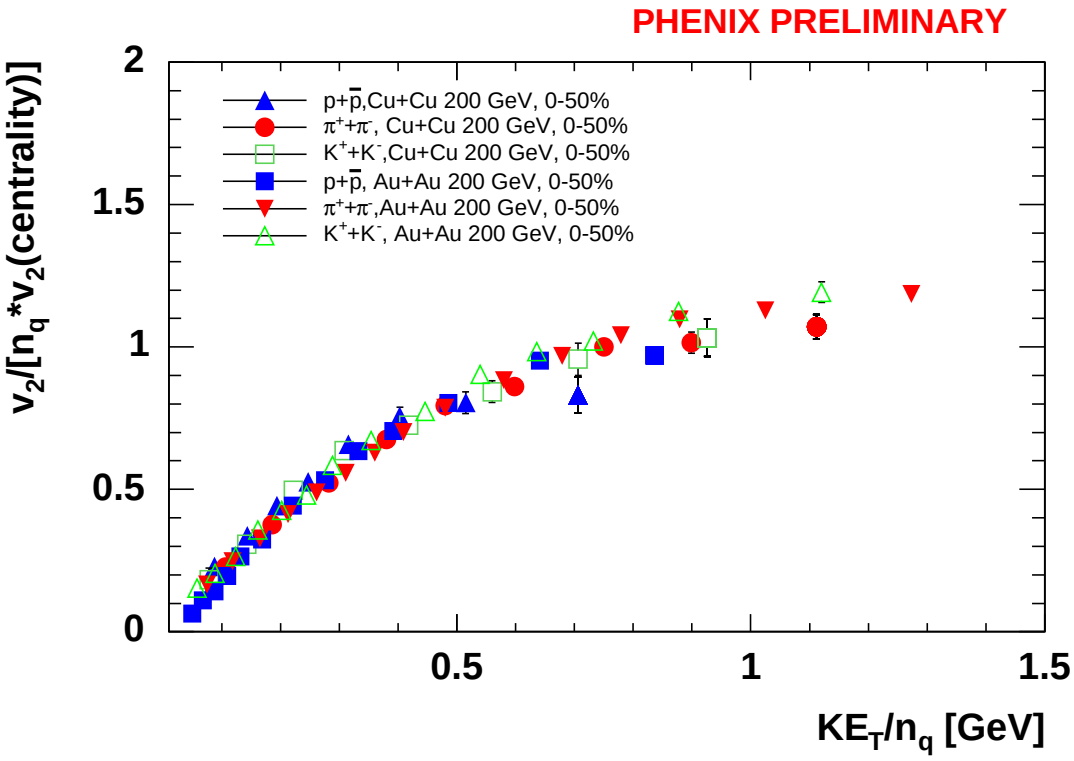

FIG. 24: v_2/n_q vs KE_T/n_q for $\pi^{\pm}$, $K^{\pm}$ and p($\bar{p}$) from central Cu+Cu and Au+Au collisions at $\sqrt{s_{NN}}$ =200 GeV scaled by the integral elliptic flow of charged hadrons measured in pt range 0.3-3.0 GeV/c)

[1] A. Adare [PHENIX Collaboration], "Scaling properties of azimuthal anisotropy in Au + Au and Cu + Cu collisions at s(NN)**(1/2) = 200-GeV," arXiv:nucl-ex/0608033.
[2] A.M. Poskanzer and S.A. Voloshin, Phys.Rev.C58:1671-1678,1998
[3] J-Y. Ollitrault , nucl-ex/9711003
[4] PPG062 data points: /phenix/WWW/p/info/ppg/062/data
[5] A. Taranenko et al., "Scaling Properties of the Azimuthal Anisotropy in Au+Au and Cu+Cu collisions at 200 GeV", PHENIX AN 441
[6] H. Masui et al., "Azimuthal anisotropy (v_2, v_4) of identified hadrons in Au+Au and Cu+Cu collisions at $sqrts_{NN}$ = 200 GeV", PHENIX AN 445
[7] H. Masui et al. "Centrality dependence of v_2 of pi,K,p from Au+Au collisions at 200 GeV, Analysis Note /WWW/p/draft/masui/2006/QM2006/analysis_note